

# Flexible and transparent moisture getter film containing zeolite

Chien-Sheng Wu · Jung-Yu Liao · Shun-Yi Fang ·  
Anthony S.T. Chiang

Received: 13 July 2009 / Accepted: 13 October 2009 / Published online: 22 October 2009  
© Springer Science+Business Media, LLC 2009

**Abstract** Organic light-emitting devices (OLED) are extremely sensitive to moisture and oxygen. Without high-performance hermetic seals, the life of these devices will be limited. A large amount of desiccant has been used in the packaging of OLED to ensure a dry environment. However, for top-emitter OLEDs, particularly for active matrix displays where the OLEDs are directly integrated on top of a thin film transistor (TFT) layer, the light must pass through a transparent encapsulating layer above the OLED, leaving little room to house the desiccant. Thus, a transparent layer with embedded moisture getter, such as zeolite, would be desirable. Here we report an effort to prepare such a transparent composite film containing zeolite nanoparticles, and show that such architecture is indeed possible.

**Keywords** Moisture getter · OLED · Nano-composite · Zeolite · Transparent

## 1 Introduction

Organic light-emitting devices (OLED), due to its self-luminescence and high contrast, have recently attracted

much attention as a device to replace the current liquid crystal displays (LCDs). OLED do not require back lighting, and can be fabricated into lightweight, thin and flexible displays. A typical OLED is constructed by placing a stack of organic electroluminescent and/or phosphorescent materials between a cathode layer that can inject electrons and an anode layer that can inject holes. When a voltage of proper polarity is applied, holes injected from the anode and electrons injected from the cathode combine and release energy as light, thereby producing electroluminescence.

The organic electroluminescent materials employed in such device are however extremely sensitive to moisture and oxygen. In order to achieve a reasonable lifespan, the device must be encapsulated in high-performance hermetic seals. The gas barrier ability of the encapsulation has been one of the major issues in the development of OLED devices. Since completely impermeable encapsulation is still impossible, a large amount of desiccant, such as calcium oxide or active alumina, is encapsulated within the device to prolong the lifespan of the device.

Zeolite is another well known desiccant materials, and has been used in the fluorescence light as early as 1927 (MacRate 1927). Zeolite-resin composite desiccant had appeared in electronics from 1990 (Shores 1993, 1994, 1997), while Sud-Chemie AG developed a zeolite based moisture getter for OLED in 2006 (Erdmann et al. 2006). However, the transparency or the flexibility of the desiccant was never an issue until the development of top emitting OLED (TOLED) device.

Traditional Bottom-emitter (Substrate side emitting) OLED is sealed via epoxy between a glass substrate and nontransparent back lid, where a large amount of desiccant could be fitted in. A top emitting OLED, on the other hand, has a relatively transparent top electrode, through which the

---

**Electronic supplementary material** The online version of this article (<http://dx.doi.org/10.1007/s10450-009-9196-3>) contains supplementary material, which is available to authorized users.

---

C.-S. Wu · S.-Y. Fang · A.S.T. Chiang (✉)  
Department of Chemical & Materials Engineering,  
National Central University, Chung-Li, Taiwan 32001, ROC  
e-mail: [Stchiang@cc.ncu.edu.tw](mailto:Stchiang@cc.ncu.edu.tw)

J.-Y. Liao  
Material and Chemical Research Laboratories,  
Industrial Technology Research Institute, Hsinchu, Taiwan 31040, ROC

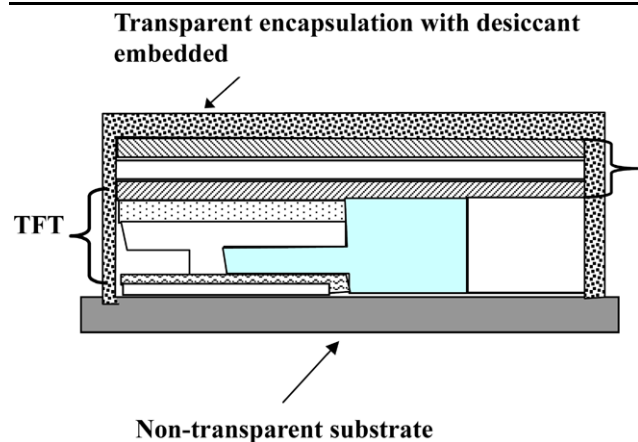


**Fig. 1** Schematics of active top-emitting OLED. (Not to scale)

emitted light emitted goes into the environment. An important application of the top emitting device structure is to achieve a monolithic integration on a polycrystalline or amorphous silicon thin film transistors (TFT) that enable an active matrix displays, as sketched in Fig. 1. The top emitting OLED structures therefore increases the flexibility of device integration and engineering, and is expected to be the leading technology for flexible displays. However, there is now little room left for the addition of desiccant or moisture getter. The problem may be partially resolved if one could have a transparent and flexible moisture getter which can be fitted between the top encapsulation and the electrode without obstructing the light. An obvious choice would be a composite of adsorbent nanoparticles and polymers. A composite moisture getter layer might become transparent if the particle size of the adsorbent is below a quarter of the visible light wavelength, or if its refractive index matches that of the matrix. Here we will present a study for the preparation of a transparent and flexible organic/inorganic nanocomposite with Beta zeolite nanoparticles and acrylic resin, and demonstrate its potential as moisture getter film

## 2 Experimental

The beta zeolite nanoparticles were prepared from a clear sol made of tetraethyl orthosilicate (TEOS), aluminum isopropoxide (AIP), Tetraethylammonium hydroxide (TEAOH) and water at a molar ratio of 1 TEOS : 0.04 AIP : 0.36 TEAOH : 25 H<sub>2</sub>O. AIP was first dissolved in 35% TEAOH then diluted with water before the drop wise addition of TEOS. As the TEOS hydrolyzed, the pH value continuously decreased and finally reached 12.82 when all TEOS was hydrolyzed into a clear sol. It was then concentrated by a rotary evaporator to ~29.5 wt% in terms of SiO<sub>2</sub>, as described previously (Hsu et al. 2005) for the synthesis of pure silicate MFI nanoparticle. The transparent viscous sol obtained was

heated in a PP bottle at 90 °C for 110 hrs until the appearance of Tyndall scattering. It was transferred to a TEFLON lined autoclave for hydrothermal reaction at 160 °C for 6 hrs. A yellowish semi-transparent sol was obtained, which was diluted to about 4 wt% and centrifuged at 23000 rpm (Beckman Avanti J-E) to separate the crystalline zeolite nanoparticles from the amorphous part.

The centrifuged products were confirmed to be beta zeolite by XRD (not given) and FTIR (Jasco-410) analysis. The materials remaining in the supernatant was X-Ray amorphous. The best crystalline yield we could achieve was about 50%. According to the ICP (JOBIN YVON JY240) analysis, the Si/Al ratio of the beta zeolite obtained was 18.9. This is slightly lower than the Si/Al = 25 recipe used, indicating that the Si/Al ratio in the amorphous part would be higher than 31. Gel with higher Si/Al ratio is more difficult to crystallize (Mintova et al. 2006). This may be the reason for the low crystalline yield.

The zeolite nanoparticles were then dispersed in aqueous Nitric acid at a pH = 1.81 and centrifuge again to remove the surface attached TEA<sup>+</sup> template. The occluded template in the zeolite pores was then oxidized at low temperature following the literature approach (Melian-Cabrera et al. 2005) using Fenton reagents. Two repeated treatments of Fenton reagents, lasted for 3 hr and 30 hr respectively, were needed to completely remove the occluded template. The template-free nanocrystals were then exchange with sodium ions in 1 M NaCl solution at 90 °C, and finally washed with IPA before surface modification.

Methacryloxy-propyltrimethoxysilane (MPTMS) was employed as the capping agent on the beta zeolite nanoparticles to facilitate the blending with acrylic resins. The grafting of MPTMS was conducted in toluene under reflux condition (110 °C/3 hr). The amount of MPTMS employed was 1 mmol/g zeolite. The modified zeolite was collected by centrifuge and washed twice with methanol, and finally dispersed in MEK for later compounding with acrylic resins. The composite was prepared by adding the MEK dispersed zeolite to a commercial hard coat solution containing roughly 37 wt% acrylic monomer and oligomers, 22.4 wt% silica nanoparticles, 5.6 wt% UV initiator and the balance MEK. Both the original composite and the zeolite added composite were coated on glass plate with doctor blade of 100 µm gap, and UV cured. The cured film was peeled off for the adsorption measurement. The composite films were baked at 200 °C, their maximum working temperature, for 12 hrs before degassed at the same temperature for 24 hr under less than 10 Pa vacuum prior to the adsorption measurement. For comparison, two beta zeolite powders were also tested. The sample before silane modification was activated at 450 °C for 24 hr. The sample after silane modification was degassed following the same protocol as the composite film. The water adsorption isotherm was measured by volumetric adsorption equipment (Micromeritics ASAP2020).

The temperature was maintained at 27 °C. The dosage was 1 STP cc/g sample and the equilibration interval for each dosage was set at 20 sec.

### 3 Results and discussion

Shown in Fig. 2 are the IR spectra of the samples at different process stages. The as synthesized beta zeolite contain TEA<sup>+</sup> template, which can be identified by the absorptions of –NH and –CH<sub>3</sub> at 1400 and 1480 cm<sup>–1</sup>, respectively. The first dosage of the Fenton reagent was not able to remove all of the occluded templates, as these peaks still existed. Only after a second dose of Fenton reagents and reacted over a longer period of time could the 1480 cm<sup>–1</sup> peak be removed, but a weak amine peak still remained. This peak probably came from the NH<sub>4</sub><sup>+</sup> cation that was produced from the decomposition of the TEA<sup>+</sup> template and resided in the zeolite cages to balance the charge of the framework aluminum. Consequently, this peak was finally removed after the exchange with sodium ion. However, the intensity of the 1640 cm<sup>–1</sup> peak, corresponding to the adsorbed water, increased after the ion exchange process. This was understandable since the bulkier NH<sub>4</sub><sup>+</sup> ion had been replaced by the smaller sodium ion. After the silane treatment, a new peak appeared at 1700 cm<sup>–1</sup>, which was the result of the grafted methacrylic function group. Since part of the surface is now covered with silane, the amount of adsorbed water was reduced as indicated by the reduction of the 1640 cm<sup>–1</sup> peak intensity. Clearly, the process of silane grafting was not complete, as there were still hydrophilic sites remaining. Notice also that the characteristic absorptions of beta zeolite at 520 and 570 cm<sup>–1</sup> were distinct peaks for the as-synthesized sample, but became broaden and overlapped after the Fenton reagent treatment. This suggests that, although the oxidative removal of templates occurred at low temperature, the structure of the beta zeolite was nonetheless affected.

The removal of occlude template could also be confirmed by the thermal gravimetric analysis (Perkin Elmer TAC 7/DX) shown in Fig. 3. According to Cambor et al. (1998), the weight loss below 350 °C could be assigned to the loss of water and the decomposition of the adsorbed TEA<sup>+</sup>, while that after ~350 °C were assigned to the two stage combustion of the TEA<sup>+</sup> balancing the framework Al(OSi)<sub>4</sub><sup>–</sup> species. For our sample, the Si/Al ratio was about 19, corresponding to ~3.2 Al<sup>+</sup> per unit cell, or ~110 mg of TEA<sup>+</sup> per gram of zeolite. The extra weight loss observed in this temperature range may be attributed to the decomposition residues left from the lower temperature. According to this and the IR analysis, the first Fenton reagent treatment could only remove the physically adsorbed templates, but had little effect on those electrostatic attached TEA<sup>+</sup> inside

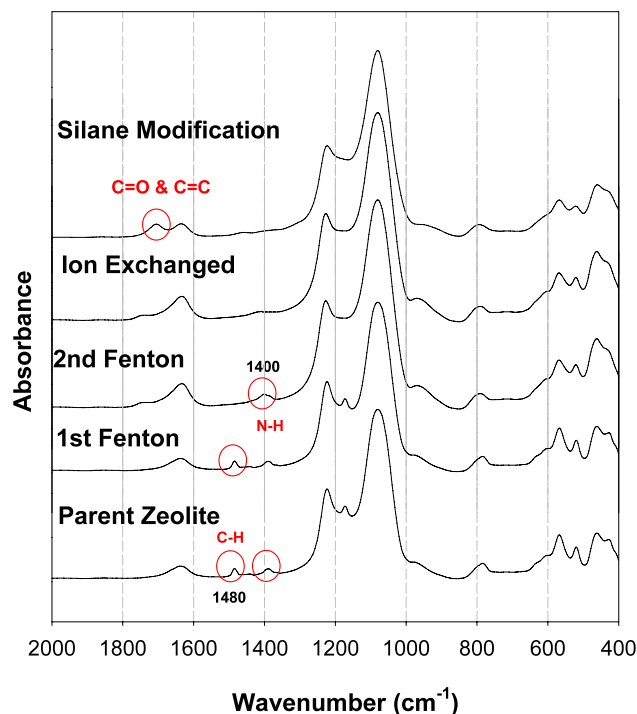


**Fig. 2** IR spectra of the beta zeolite nanoparticles at different stages of the synthesis process

the framework, which required a long period of reaction after the second dose of Fenton reagent.

The particle size distribution (DLS particle size, Malvern Nano-ZS) of the sample at different stages of the process is displayed in Fig. 4. The as-synthesized sample had a very narrow size distribution around 50 nm, which did not alter much after the low temperature Fenton reagent and the ion exchange treatments. The polydispersity index (PDI) of the as-synthesized and the template-removed samples were 0.11 and 0.14, respectively, indicating a reasonable monomodal particle size distribution. However, these particle size distributions were measured as aqueous dispersion, while the preferred solvent for blending the nanoparticles and the acrylic resin is MEK. It was impossible to disperse the template-removed zeolite nanoparticle in MEK before grafting of MPTMS. Unfortunately, as shown in Fig. 4, two size fractions are observed after silane grafting, and the PDI increased to 0.3, signifying the occurrence of some agglomerations. The larger agglomerates were about 180 nm in size, roughly a collection of 10 original nanoparticles. Nevertheless, since the size distribution in Fig. 3 was plotted in terms of scattering intensity, which increases with the sixth power of particle size, the actual volume percentage of the larger agglomerates should be much smaller than suggested in the figure, thus a transparent nanocomposite was still possible, as demonstrated by the UV-Vis spectra in Fig. 5.

The room temperature water adsorption isotherm of the beta zeolite nanoparticles was given in Fig. 6A. In here two

**Fig. 3** Thermal gravimetric analysis results of the beta zeolite nanoparticles at different stages of the synthesis process

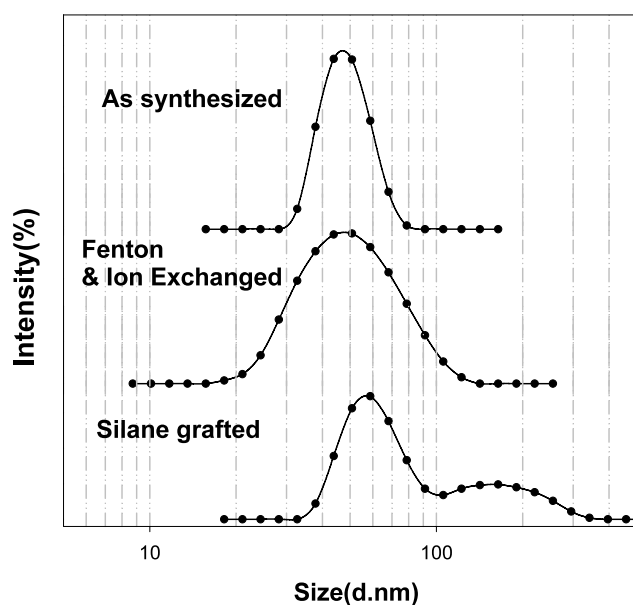
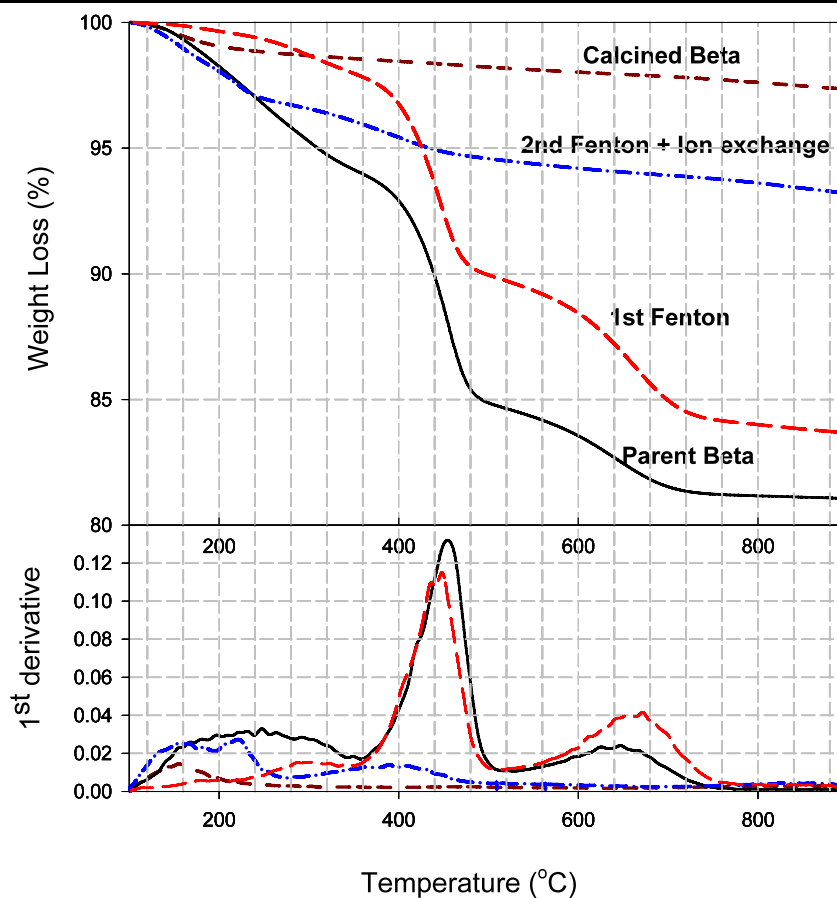


**Fig. 4** DLS particle size distributions of the beta zeolite nanoparticles at different stages of the preparation process. The as synthesized and the ion exchanged samples were measured as aqueous dispersion, while the silane grafted sample was measured as MEK dispersion

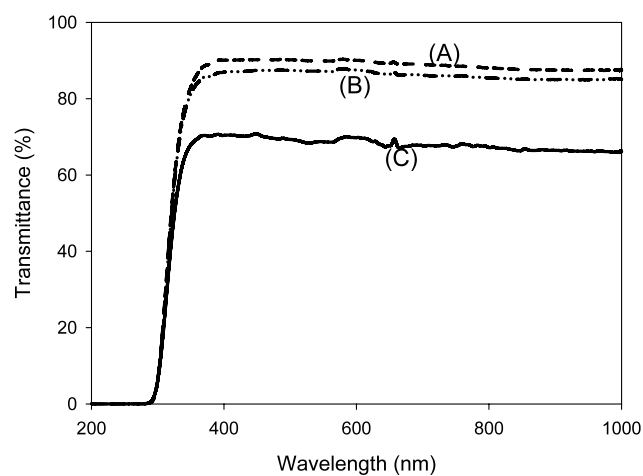


**Fig. 5** UV-Vis spectra of the glass slides coated with the original hard coat sol (A), composite sol containing 9.8 wt% of zeolite (B) and composite sol containing 28.4 wt% of zeolite (C). The film thickness was about 50  $\mu\text{m}$

sets of isotherm data were showed, corresponding to the two different degassing conditions. The amount of water adsorbed was also compared to the literature (Bolis et al. 2006) value of beta zeolite (large crystal  $H\beta$ ,  $\text{Si}/\text{Al} = 9.8$ , 600  $^{\circ}\text{C}/2\text{h}$  activation) as listed in Table 1.

**Table 1** Water adsorption capacity of the modified beta nanocrystals, the resin and the composite

	Degas temp. (°C)	Degas duration (hr)	@ 0.5 torr (mg/g)	@ 5 torr (mg/g)
<i>n</i> -Na $\beta$ (Si/Al~19)	450	24	46.8	104
<i>n</i> -Na $\beta$ (Si/Al~19) silane modified	200	24	20.5	51
Bolis et al. 2006 (Si/Al = 9.8)	600	2	42.8	89
Original hard coat film	200	24	1.6	10
Hard coat film with 10 wt% (dry base) silane modified <i>n</i> -Na $\beta$ zeolite added	200	24	2.5	14

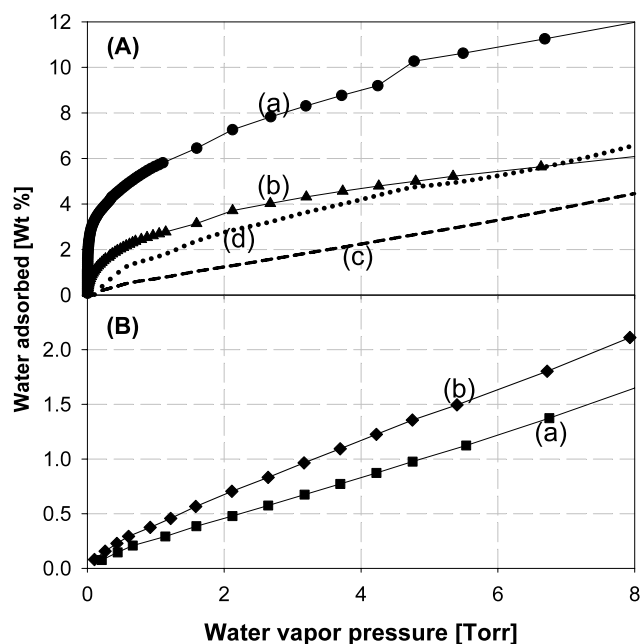


**Fig. 6** 27 °C water adsorption isotherms of the Na-beta zeolite nanoparticles degassed at 450 °C for 24 hrs (A-a), silane modified Na-beta zeolite nanoparticles activated at 200 °C for 24 hrs (A-b), calculated isotherm for imbedded silica in the original hard coat film (A-c), and specific adsorption capacity of the imbedded zeolite in the modified hard coat film (A-d). Water adsorption isotherms of the original hard coat film (B-a) and that of the zeolite added hard coat film containing 10 wt% zeolite on dried base (B-b)

It was found that only after vacuum activation at 450 °C could we reached the water adsorption capacity reported in the literature. Under this condition, our sample had in fact a slightly higher capacity, despite of a much smaller crystal size. This may have come from the fact that a sodium exchanged form was used here instead of the hydrogen form. However, for the silane modified nano-zeolite, where the degassing temperature was limited to 200 °C, the water adsorption capacity was almost halved compared to that unmodified zeolite degassed at 450 °C. The reason we tested the low

temperature degassing condition was that, when the zeolite was silane grafted and embedded in acrylic resin, the maximum working temperature will be 200 °C. Thus it was necessary to establish the adsorption capacity of the low temperature degassed sample.

Although it is believed that the observed difference in adsorption capacity came mainly from the change in activation temperature, one can not preclude the effect of the hydrophobic motifs grafted onto the surface after silane modification. However, this is a price we have to pay in order to make the zeolite compatible to and fully dispersible in the hydrophobic acrylic resin. Without such modification, a transparent composite film would be impossible. Fortunately, according to the above results, at least half of the adsorption capacity could be retained even after silane modification and activated at a limited temperature. The remaining question is whether such a composition meets the practical requirements on a moisture getter.

According to its composition given in the experimental section, the film produced by the hard coat solution contains about 37 wt% silica nanoparticles. Although not as effective as zeolite, these embedded silica particles also adsorb water. Thus, as exhibited in Fig. 6B(a), there is a reasonable moisture adsorption capacity for the hard coat film even before adding zeolite. If we assumed that the polymer part in the hard coat film contributed nothing to the adsorption of moisture, we could calculate the specific water adsorption capacity of the embedded silica, which is plotted as the dash line (c) in Fig. 6A. It is clear that under the same activation condition, the embedded silica is far less effective a moisture adsorbent than the silane modified zeolite.

By the addition of only 10 wt% zeolite into the hard coat film, a substantial increase of the water adsorption capacity was observed in Fig. 6B(b). The actual contribution of the added zeolite could be deduced by subtracting the capacity of the zeolite free hard coat film. The result was plotted as dotted line (d) in Fig. 6A. It is observed that the specific capacity of the embedded zeolite is just slightly lower than



that measured with silane modified powder activated under the same condition. Therefore, the acrylic matrix did reduce the water adsorption capacity of the embedded zeolite but not to a great extent.

Based on the above results, a rough estimation of the required moisture getter compositions can be made. With the current technology, a gas barrier film with water permeation less than  $10^{-3}$  g/m<sup>2</sup> day is easily achievable, although still about three orders of magnitudes away from acceptable for OLED packaging. To remove the amount of water penetrated in 10 years of expected product life, the required moisture getter capacity would be about 3.6 g/m<sup>2</sup>, or 0.37 mg/cm<sup>2</sup>, which was the reported value of commercial nontransparent moisture getter (SAES Dryflex, ~130 µm) (SAES Getters 2006). If this was expected on a 100 µm thick transparent getter film, the water adsorption (absorption) capacity would have to be about 3 wt%, assuming a composite density of ~1.2 g/mL. Based on the above adsorption data, one must include at least 50 wt% of zeolite in acrylic matrix to achieve such capacity at below 1 torr water vapor pressure. The challenge however should be to keep the transparency and processibility of the composite at such a high zeolite loading.

Currently, the best we could achieve in a transparent composite is ~20 wt% in zeolite loading, as demonstrated in the picture given in the supporting information. To further increase the zeolite loading without hampering the transparency, a better control of the particle size distribution must be achieved, in particularly during the silane modification step. Clearly, if we were to expect higher water adsorption capacity with less zeolite loading, the zeolite must be fully dehydrated before silane grafting, and the following surface modification, compounding and coating must all be done in a moisture-free condition until the completion of the packaging process. Luckily, such moisture free operations are the standard practice in the OLED packaging industry. As demonstrated by our data, the adsorption capacity of 450 °C degassed zeolite is at least twice of that degassed at 200 °C. A substantial improvement could be achieved if the silane grafting, resin compounding and the OLED encapsulation steps could all be performed in a moisture-free environment right after the activation of zeolite at high temperature.

Based on such expectation, the transparent composite moisture getter film having only 20% zeolite might already be enough to prolong the life of an OLED device to more than 4 years. Such an expected life span would be acceptable in some commercial applications.

## 4 Conclusion

Making zeolites into nanoparticles enables the extension of its old application as desiccant into new domains. Unlike the traditional adsorption process, where one is more concern with the regeneration and process efficiency, new applications may put more emphasis on how to place the required adsorbent in the right position and having other functions. Similar situations may also be true for other adsorbents such as active carbons and the likes.

## References

- SAES Getters: DryFlex data sheet (2006). [www.seasgetters.com](http://www.seasgetters.com)
- Bolis, V., Busco, C., Ugliengo, P.: Thermodynamic study of water adsorption in high-silica zeolites. *J. Phys. Chem. B* **110**(30), 14849–14859 (2006)
- Cambor, M.A., Corma, A., Valencia, S.: Characterization of nanocrystalline zeolite beta. *Micropor. Mesopor. Mater.* **25**(1–3), 59–74 (1998)
- Erdmann, E., Schall, N., Kirtikar, A.: Getter paste for OLED application. *SID digest*, P-63 (2006)
- Hsu, C.Y., Chiang, A.S.T., Selvin, R., Thompson, R.W.: Rapid synthesis of MFI zeolite nanocrystals. *J. Phys. Chem. B* **109**(40), 18804–18814 (2005)
- MacRate, D.: Getter and method of applying the same. Westinghouse Lamp Co. US patent 1,626,682 (1927)
- Melian-Cabrera, I., Kapteijn, F., Moulijn, J.A.: Room temperature de-templation of zeolites through H<sub>2</sub>O<sub>2</sub>-mediated oxidation. *Chem. Commun.* **21**, 2744–2746 (2005)
- Mintova, S., Valtchev, V., Onfroy, T., Marichal, C., Knozinger, H., Bein, T.: Variation of the Si/Al ratio in nanosized zeolite veta crystals. *Micropor. Mesopor. Mater.* **90**(1–3), 237–245 (2006)
- Shores, A.A.: Enclosure for electronic devices. US patent 5,244,707 (1993)
- Shores, A.A.: Moisture and particle getter for enclosures. US patent 5,304,419 (1994)
- Shores, A.A.: Moisture getting composition for hermetic microelectronic devices. Alpha fry limited. US patent 5,591,379 (1997)